Petroleum and Coal

Article **Open Access**

Coal Geochemistry for Determining the Quality and Depositional Environments of Coal-Forming Mire System, A Case Study

Abu-Bakr R. Abdel-Fatah[1] & Nader A. A. Edress[2]

[1] *El-Nasr Company for Coke and Chemicals Industry, Helwan, Cairo, Egypt*
[2] *Department of Geology, Faculty of Science, Helwan University, Helwan, Cairo, Egypt*

Received July 11, 2021; Accepted January 14, 2022

Abstract

Selected Jurassic-Cretaceous bituminous coal seams in the Crowsnest coalfield, Southeast British Columbia, Canada were investigated, as a case study, for comparing their quality and mineral geochemistry, as a function of their Paleo-depositional environments. Twenty-two channel coal samples were collected from the base (S10) coal seam and the top (SC) coal seam of the Mist-Mountain Formation in the Crowsnest Coalfield. Ash, Gross Calorific Value (GCV), Volatile Matter (VM), Fixed Carbon (FC), are measured to determine the quality of the studied coal seams. The obtained results defined the coal seam (S10) as a bituminous rank group of low-volatile bituminous according to the ASTM standard (Ash= 13.21% db; GCV= 34.3 MJ/KG mmmf; VM=19.3% dmmf; FC= 80.7% dmmf). Whereas, the studied coal seam (SC) is postulated to be a bituminous rank group of high-volatile bituminous class- (A) (Ash= 8.26% db; GCV= 35.2 MJ/KG mmmf; VM= 31.14% dmmf; and FC= 68.86% dmmf). Ten samples are investigated the major and minor oxides, six samples for trace elements and mineral assemblages of coal samples, using X-ray fluorescence spectrometry and X-ray diffraction XRD techniques. Ashing geochemistry indicates domination of kaolinite and quartz minerals associated deposition of coal seams. The Palaeoclimatology was fully humid and warm. The deposition was acting under suboxic to dysoxic conditions. Water feeding was absolutely rain and riverine of freshwater origin. The catchment mire system was located within an active margin province that surrounding by a hinterland area composed of intermediate igneous rocks that were subjected to intensive chemical weathering.

Keywords: *Geochemistry; Coal-forming environment; Mist-Mountain formation; Canada.*

1. Introduction

Canada is one of the biggest countries in coal-producing all over the world. Approximately half of its production is shipping worldwide, essential for the thermal and metallurgical industry [1]. The origin of Mesozoic-Early Tertiary Canadian coal basins began with a convergence tectonic activity formed by the collision of the North American Plate and the Pacific plate, which was dated Middle to Late Jurassic time and continued till Early-Tertiary. This collision caused the formation of a huge fore-deep basin. Enormous accumulation of wedge-shaped sediments (≈ 2700 m), containing economic coal-bearing strata [2-4]. The Mist-Mountain Formation of the Kootenay Group is considered the essential coal-bearing strata of the entire succession. It is exposed along within three substantial isolated structures which extend about170 km along the southeastern border of British Columbia, Fig. (1). Elk-Vally, Crowsnest, and Flathead structural terrains are forming together the so-called East-Kootenay basin [5]. The composite section of the Mist-Mountain formation reaches 600-650 m in thickness vertically and involves 48 coal seams in the Elkview mine at the northern part of the Crowsnest area [6-7], from which only 11 coal seams are of economic interest. The coal seams range in thickness from 0.9 m to15.6 m embody ranges between 8% to 12% of the total stratigraphic thickness of the formation [8-12].

The current work is attempting to shed the light on the benefits of geochemical analysis either organic or inorganic to identify the quality and Paleo-mire system of two studied coal seams from the Crowsnest mining area at the base (S10) and at the top (SC) to give facts on Paleo-environmental and geological conditions during the deposition of the precursor major mire system including climatology, type of water feeding, redox potential, the intensity of weathering, and general tectonic setting. Depositional Paleo-environments are carried out based on ratios of the abundance and distribution of major minerals and trace elements comprises studied coal seams ash.

2. The geological setting

The Crowsnest coalfield is pear-shaped, cored by the younger Early Cretaceous Elk Formation, and almost completely rimmed by outcrops of the older coal-bearing Jurassic-Cretaceous Mist-Mountain Formation. About 50 km long, 20 km wide, occupies approximately 600 square kilometers in size. The coalfield occupies a structural synform depression referred to as the Fernie Basin, extends from southeast of Fernie to north of Sparwood town, and lies in the general vicinity of the Crowsnest Pass [13]. The studied coal section lies at the extreme north of the Crowsnest coalfields. It lies across latitude 49.7345°N and longitude 114.879°W, approximately three kilometers east of Sparwood town in an open-cast mining area (Elkview) (Fig.1). The Crowsnest region displays three categories of coal-seams ranks as a function of their burial depth and geothermal gradient in the basin. It started with a low-volatile bituminous coal seam at the base, which gradually is overlain by a medium-volatile bituminous one. Finally, it is topped by a high volatile bituminous coal-seam. Both low and medium volatile coal-seams in the study area are related to the Late-Jurassic time. The uppermost high-volatile coal-seams within the same formation are of Early-Cretaceous age [14-15].

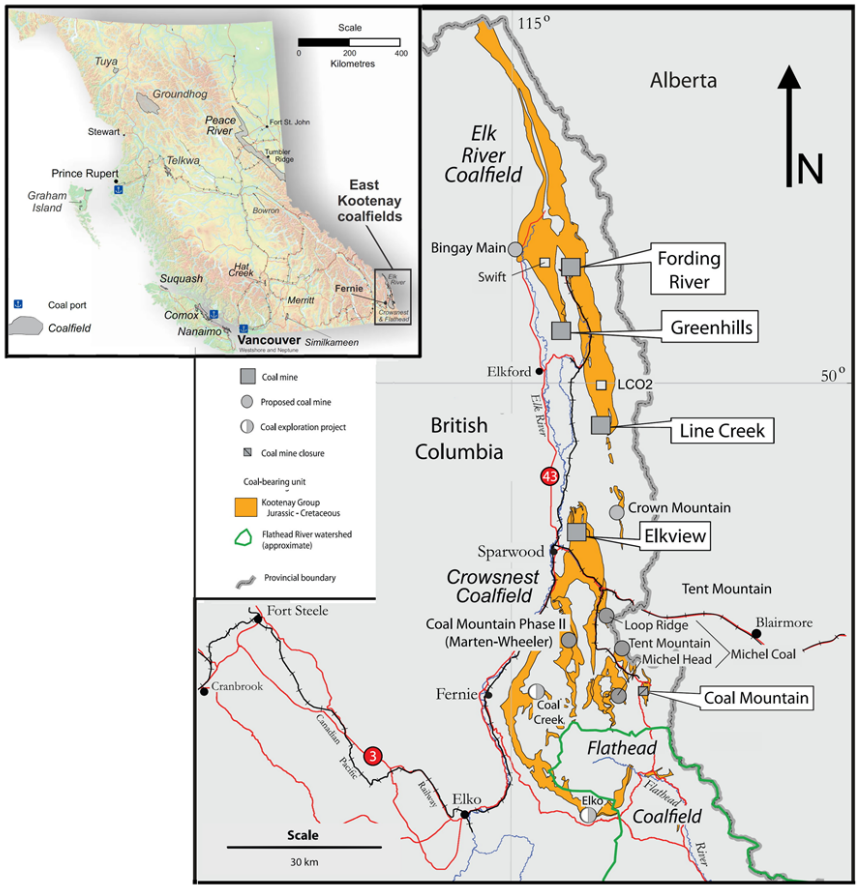

Fig. 1. Location map of the study area

2.1. Stratigraphy

In the study area, the Mist-Mountain Formation reaches 665 m in thickness, It is composed of a clastic sequence comprising an interbedded succession of sandstone, siltstone, mudstone, rare conglomerates and economically important seams of cumulative coal over 60 m (Fig. 2). It forms a broad syncline, the rims of the fold contain the younger coal-bearing strata, where the older coal is being at the core that covered by the younger Elk Formation and conformably overlies the Moose Mountain Member of the Morrisey Formation.

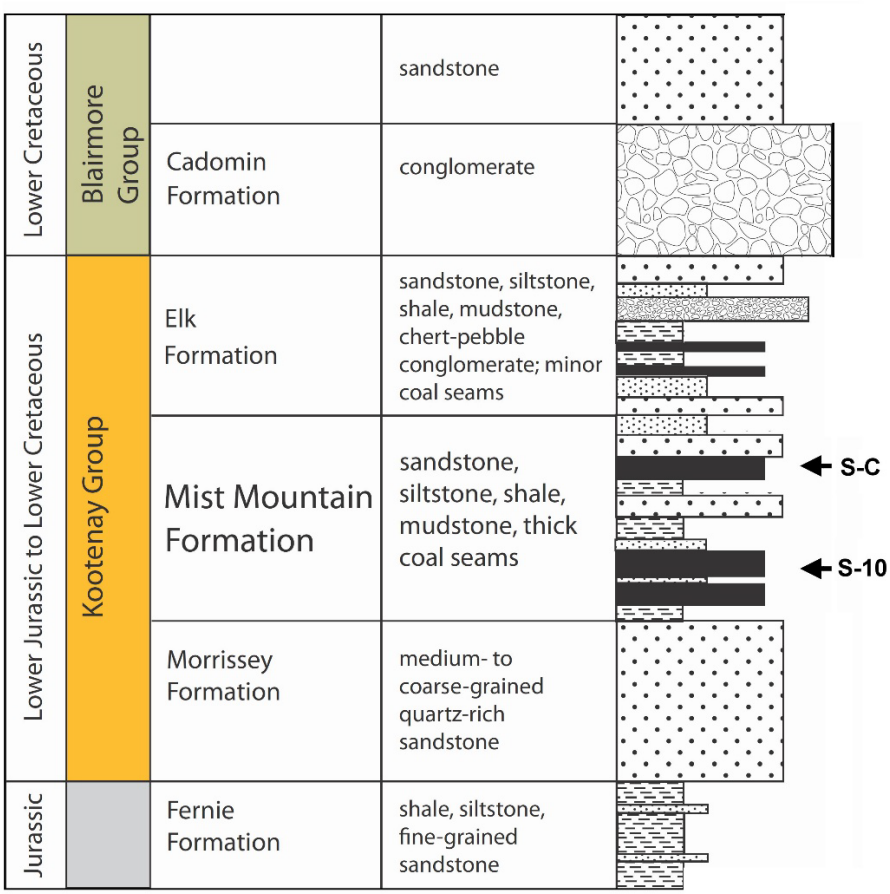

Fig. 2. Composite stratigraphic column of coal-bearing formation in north Crowsnest mining area [16]

2.2. Structural setting and tectonics

The coal-bearing strata in the study area formed during the first stage of three stages of global tectonic activity. These compressional stages began at Jurassic till the Early-Tertiary periods mentioned in Columbia-1, Columbia -2, and Laramide. The periods of these stages are Jurassic to Early-Cretaceous; Early to Late-Cretaceous, and Late-Cretaceous to Tertiary time in respective order [3, 10, 15].

2.3. Methods

Ten channel samples were collected from approximately 15 m of the (S10) coal seam and twelve samples were obtained from 5 m of the (SC) coal seam from the Mist-Mountain Formation at Crowsnest mining area. The samples were numbered and ordered from base to top numerically. The picking up of coal samples are carried out under the permission of Teck Resources limited that collected and delivered two boxes (20 kg) of each S10 and SC coal seams by shipping transport associated with the imported annual package of coking coal to El-Nasr Company in Egypt for academic researches.

Some coal samples are pulverized to 250 microns (100 mesh) for fuel analysis of proximate, ultimate, and calorific values at the Chemical Laboratory of El-Nasr Coke Company in Egypt. The standards of analytical methods [17-18] were applied and the automatic analyzer instrument (Vario-Elementar) was used to determine the C, H, N and S contents at the Micro Analytical Center (MAC) in Cairo University. The form of sulfur in coal samples was measured by the combustion method using a tube furnace ASTM standard [19]. Ten coal samples from the two studied seam sections (SC and S10) were used for this investigation. Each sample was ground to a fine powder (< 212 μm), split into representative portions for further analyses. The percentages of major oxides (SiO_2, TiO_2, Al_2O_3, Fe_2O_3, MgO, CaO, MnO, Na_2O, K_2O, and P_2O_5) for each sample after ashing were determined by an X-ray fluorescence spectrometer (Shimadzu MXF-2400, XRF) at Egyptian Iron and steel company. The powder samples of the studied seams were subjected to low-temperature ashing (LTA) at 370 ^{0}C analyzed by PAN analytical X-Ray Diffraction equipment model X'Pert PRO with a monochromator, Cu-radiation (1.542 A^o) at 45 K.V. and scanning speed 0.03^o/sec using Siroquant-Rietveld software for semi-quantitative mineralogical analysis. Losing ignition (LOI) was also determined at this temperature by the gravimetric method. Trace elements of coal samples powder (< 74μm) were analyzed by X-ray fluorescence equipment PW 2404. The trace elements and XRD procedures are performed at the Egyptian Mineral Resources Authority, EMRA.

3. Results and discussion

3.1. Coal seams quality and chemistry

3.1.1. Proximate analysis

The amounts of moisture, volatile matter, ash yield, and fixed carbon were measured for each coal sample (Tables 1 & 2). Moisture in coal is a basic parameter for evaluating the economic value of coal, and it is a useless constituent, especially in coal combustion. As the depth increases, the moisture decrease, but this phenomenon is not to be applicable for all coal types and all different circumstances [20]. The studied coal shows a reverse relationship between moisture and depth. The lower coal seam (S10) has moisture of 2.03%, which is higher than the younger upper coal seam (SC) with average moisture content equals 1%. Sivek *et al.* [21] mentioned one of many important reasons for increasing the moisture content with depth that may be attributed to the structure change of the coal itself during the progress of coalification. Based on the previous author assumption agreements with the present coal samples, the coal seam (S10) reaches an initial stage of semi-anthracite coalification that may change in its structure and lead to add up additional moisture more than the coal seam (SC) plus other factors of increasing moisture like tectonic structures, precursor vegetation types, a mineral associated, hydraulic activity, expelled methane gases, and so on.

The ash yield of coal is an important indicator for the assessment of coal quality as a coal grade. The ash in coal lowers its calorific value and gives a polluted effect to the environment during the coal combustion [22]. Consequently, the coal seam (S10) is characterized by its medium grade of ash contents (13.21% db) which is higher than the coal seam (SC) of high-grade coal with an average of ash (8.26% db), Tables (1 & 2). The MM content of both coal seams has coincided with the average values of its ash content. The average MM percentages of (S10) coal seam are 14.4% decreasing toward the younger coal seam (SC) to reach 9.21%. These significant decrease trends in ash and mineral matter from coal seam (S10) to coal seam (SC) may refer to the development of mire shape and its vegetation over time [23].

The volatile matter refers to the yield of volatile product (liquid or gas) of organic matter in coal during pyrolysis. The measured volatile matter varies from low amounts of 17.6% to 20.2% (average, 19.3% dmmf) for (S10) coal seam and high amounts of 30.86% to 31.54% (average, 31.14% dmmf) for the (SC) coal seam that confirms the affinity of the rank of low volatile bituminous for the S10 coal seam and of high volatile bituminous for the SC coal seam.

Table 1. Geochemical results of the proximate and ultimate analysis of the (S10) and (SC) coal samples; moisture (M); ash (Ash), volatile matter (VM), fixed carbon (FC); carbon (C); hydrogen (H); nitrogen (N); total sulfur (S_{total}); pyrite sulfur (S_{Pyr}); sulfates (S_{Sulf}); organic sulfur (S_{org}); as receive (ar); dry basis (db)

Sample no.		As-received basis (ar) %				Dry basis (db) %									
												Sulfur			
		M	Ash	VM	FC	Ash	VM	FC	C	H	N	S_{total}	S_{Pyr}	S_{Sulf}	S_{org}
(SC) coal seam	12	1.17	8.24	29.33	61.25	8.34	29.68	62.98	78.63	4.33	1.15	0.54	0.06	0.03	0.45
	11	1.08	7.85	29.99	61.07	7.94	30.32	61.74	76.85	4.57	1.32	0.48	0.05	0.02	0.41
	10	1.00	7.84	29.82	61.34	7.92	30.12	62.56	78.1	5.19	1.22	0.50	0.05	0.03	0.42
	9	0.88	7.89	29.35	61.88	7.96	29.61	62.43	78.82	4.78	1.27	0.48	0.04	0.02	0.42
	8	0.8	8.2	29.46	61.52	8.28	29.7	62.02	78.2	4.44	1.13	0.42	0.04	0.03	0.35
	7	1.2	7.79	29.97	61.05	7.88	30.33	61.79	76.9	5.15	1.22	0.58	0.05	0.04	0.49
	6	0.98	7.9	29.85	61.25	7.99	30.15	61.86	78.12	4.98	1.12	0.60	0.04	0.03	0.53
	5	0.92	8.39	29.25	61.44	8.47	29.52	62.01	78.2	4.77	1.19	0.54	0.06	0.04	0.44
	4	1.3	8.18	29.39	61.12	8.29	29.78	61.93	77.39	4.73	1.26	0.52	0.05	0.02	0.45
	3	0.95	8.31	29.44	61.30	8.39	29.72	61.89	77.44	4.69	1.29	0.52	0.05	0.03	0.44
	2	0.89	8.44	29.36	61.31	8.52	29.62	61.86	77.57	4.20	1.25	0.48	0.04	0.03	0.41
	1	0,87	9.06	28.22	60.85	9.14	29.48	62.38	76.15	4.69	1.07	0.60	0.05	0.04	0.51
Average		1.00	8.18	29.54	61.28	8.26	29.84	61.9	77.7	4.71	1.21	0.52	0.05	0.05	0.03
(S10) coal seam	10	2.22	13.24	17.68	66.86	13.54	18.08	68.38	79.7	4.0	1.2	0.34	0.06	0.02	0.26
	9	1.98	12.88	17.84	67.3	13.14	18.2	68.66	79.8	4.11	1.2	0.26	0.04	0.02	0.2
	8	1.77	12.63	18.66	66.93	12.86	19	68.14	78.55	3.95	1.18	0.29	0.05	0.01	0.23
	7	1.68	13.32	19.22	65.78	13.55	19.55	66.9	78.85	4.3	1.18	0.28	0.03	0.02	0.23
	6	2.00	12.94	19.33	65.74	13.2	19.72	67.08	77.55	4.25	1.32	0.32	0.04	0.02	0.26
	5	1.95	13.18	19.16	65.71	13.44	19.54	67.02	77.75	4.15	1.22	0.34	0.06	0.02	0.26
	4	2.10	12.55	19.7	65.65	12.82	20.12	67.06	78.82	4.05	0.98	0.32	0.05	0.02	0.25
	3	2.18	12.64	19.82	65.36	12.92	20.26	66.82	77.9	4.40	1.11	0.28	0.03	0.01	0.24
	2	2.22	12.71	19.54	65.53	13.00	19.98	67.02	77.62	4.06	0.71	0.27	0.04	0.01	0.22
	1	2.20	13.32	18.50	65.98	13.62	18.92	67.46	77.5	3.79	0.68	0.3	0.06	0.02	0.22
Average		2.03	12.94	18.94	66.1	13.21	19.34	67.45	78.4	4.1	1.08	0.3	0.05	0.05	0.02

Table 2. Geochemical results of the proximate and ultimate analysis of (S10) and (SC) coal samples; carbon (C); hydrogen (H); nitrogen (N); organic sulfur (S_{org}); mineral matter (MM = 1.08 Ash + 0.55 S_{total}); fixed carbon (FC); volatile matter (VM); gross calorific value (GCV)

Sample no.		MM % Parr-formula	Dry ash free (daf) %					Dry mineral matter free (dmmf) %							GCV Mj/kg
			C	H	N	S_{org}	O_2	Atomic Ratios			C	H	FC	VM	
								H/C	O/C	C/N					
(SC) coal seam	12	9.30	85.78	4.72	1.25	0.49	0.71	0.66	0.07	79.77	86.7	4.77	69.14	30.86	34.7
	11	8.84	83.48	4.96	1.43	0.45	0.8	0.71	0.09	67.92	84.3	5.01	68.46	31.54	35.8
	10	8.83	84.82	5.64	1.32	0.46	0.73	0.8	0.07	74.69	85.66	5.69	68.63	31.37	36.7
	9	8.86	85.64	5.19	1.38	0.46	0.68	0.73	0.06	72.41	88.68	5.24	69.1	30.91	35.9
	8	9.17	85.26	4.84	1.23	0.38	0.80	0.68	0.07	80.74	86.1	4.89	68.82	31.18	36.0
	7	8.83	83.48	5.59	1.32	0.53	0.76	0.80	0.08	73.54	84.35	5.65	68.58	31.42	35.9
	6	8.96	84.90	5.41	1.22	0.58	0.73	0.76	0.07	81.38	85.92	5.47	68.59	31.41	36.4
	5	9.44	85.44	5.21	1.30	0.48	0.73	0.73	0.07	76.67	86.41	5.27	69.09	30.91	34.0
	4	9.24	84.39	5.16	1.37	0.49	0.73	0.73	0.08	71.66	85.27	5.21	69.14	30.86	33.8
	3	9.35	84.53	5.12	1.41	0.48	0.65	0.73	0.08	70.04	85.93	5.17	68.91	31.09	34.4
	2	9.47	84.79	4.59	1.37	0.45	0.74	0.65	0.08	72.40	85.68	4.64	68.93	31.07	36.0
	1	10.20	83.81	5.16	1.18	0.56	0.73	0.74	0.08	83.03	85.91	5.22	68.92	31.08	34.0
Average		9.21	84.7	5.13	1.31	0.48	8.37	0.73	0.07	75.35	85.91	5.19	68.86	31.14	35.2
(S10) coal seam	10	14.8	92.18	4.63	1.39	0.3	0.62	0.60	0.01	77.49	94.49	4.69	82.35	17.6	33.6
	9	14.3	91.87	4.73	1.38	0.23	0.61	0.62	0.01	77.58	93.26	4.8	82.00	18	33.9
	8	14.05	90.14	4.53	1.35	0.26	0.65	0.61	0.03	77.66	91.85	4.59	80.89	19.1	34.22
	7	14.8	91.21	4.97	1.36	0.27	0.66	0.65	0.02	77.96	93.71	5.05	80.04	20	33.8
	6	14.4	89.34	4.90	1.52	0.3	0.64	0.66	0.03	68.54	92.97	4.97	80.21	19.8	34.6
	5	14.7	89.82	4.79	1.41	0.3	0.62	0.64	0.03	74.35	92.56	4.86	80.35	19.7	34.4
	4	14.0	90.41	4.65	1,12	0.29	0.68	0.62	0.03	93.8	91.67	4.71	79.89	20.1	35.4
	3	14.1	89.46	5.05	1.27	0.28	0.63	0.68	0.03	81.8	91.92	5.12	79.77	20.2	34.6
	2	14.2	89.22	4.67	0.82	0.25	0.6	0.63	0.04	127.5	93.95	4.73	80.13	19.9	33.7
	1	14.9	89.72	4.39	0.79	0.25	0.63	0.6	0.04	133	93.88	4.45	81.30	18.7	34.8
Average		14.4	90.34	4.73	1.24	0.27	3.42	0.63	0.03	88.89	93.03	4.8	80.7	19.3	34.3

3.1.2. Ultimate analysis

The carbon content of coal increases by the progression of the coalification process, the relative release of oxygen and hydrogen due to thermal cracking in coal leads to an increase in the amount of carbon [22]. Therefore, the studied higher rank coal seam (S10) has a high carbon content of 93.03% (dmmf), which is higher than the carbon content of the lower rank coal seam (SC) of an average carbon of about 85.91% (dmmf). By plotting, samples of the studied coal seams on Seyler's diagram (Fig. 3) show that the coal samples of S10 coal seam are at the end stage of a bituminous and initial stage of anthracite characterized by per-hydrous of high hydrogen coal where the SC coal seam are chiefly bituminous coal with ortho-hydrous and sub-hydrous characteristics of gas-prone vitrinite (Fig. 3).

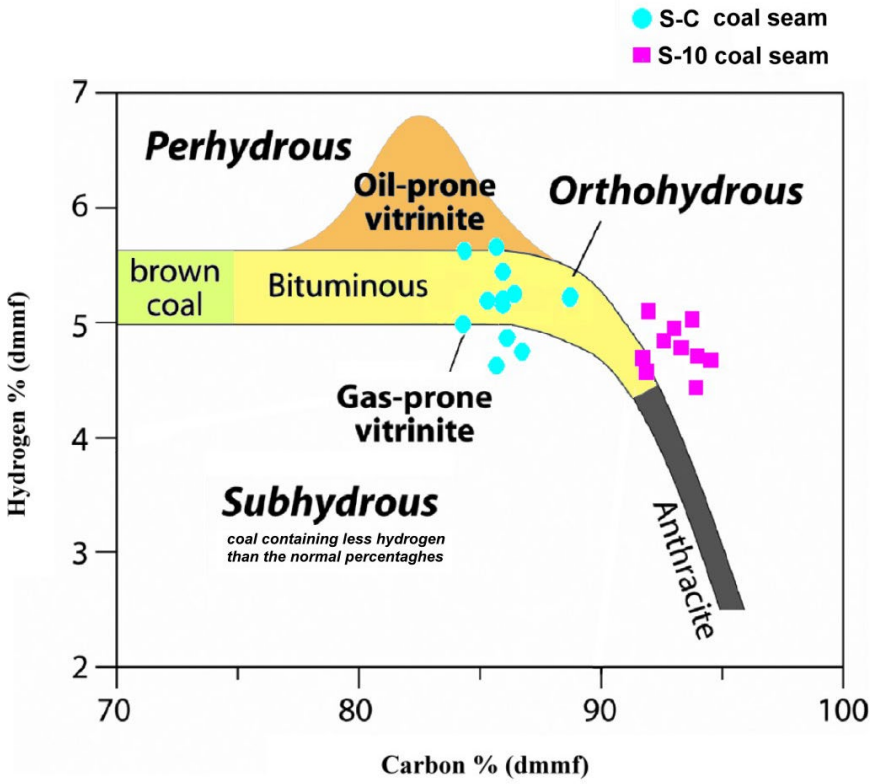

Fig. 3. Show a composition of coal and its relation to gas-prone (ortho-hydrous and sub-hydrous) against oil-prone (per-hydrous) coal [24-25]

The measured total sulfur in both studied seams displays small average values of 0.3% and 0.52% db for the coal seams (S10) and (SC) respectively. [26] and [27] suggested that the coal of the low-sulfur <1% commonly is of organic origin which is derived from the plant material accumulated in a mire of mainly freshwater feeding (non-marine). In contrast, the mire of coastal influence of seawater-coal shows an increase leads to the formation of a category of medium- to high-sulfur coals. The geochemical measurements of the present studied coal seams (S10) and (SC) show a type of coal that has low sulfur with an average amount of 0.3% and 0.52% db respectively. The depositional setting of both studied (S10) and (SC) coal seams excluded the marine-influenced coal and confirm the limnic coal Paleo-environments. The organic sulfur corresponds to 79% of the total sulfur of the (S10) coal samples and this value increases to reach 84.98% of the total sulfur amount related to the (SC) coal samples, Table (2). [28] and [29] stated that the amount of organic sulfur measured in coal may depend on types of maceral content (vitrinite, inertinite, and liptinite). They added that the amount of organic sulfur in the macerals of the vitrinite is twice higher than its amount in the macerals of the inertinite.

3.1.3. H/C ratio versus O/C ratios

Kerogen in sedimentary rocks is commonly classified according to the van Krevelen diagram, in which H/C ratios are plotted versus O/C atomic ratios. Dependent on the biological source materials, three different main types of kerogens. By Plotting the obtained results of (S10) and (SC) coal samples (Table 2) on the H/C - O/C Van-Krevelen coal genesis diagram [25] (Fig. 4) revealing the domination of Type III kerogen which is characteristic of humic organic matter with high O/C ratios and H/C ratios lower than 1.0.. Type III kerogen is the product of woody plant tissue and thus encompasses the full range of vitrinite macerals, including huminite, telinite, collinite and semifusinite. In contrast to types I and II, type III kerogen is recognized as a limited oil generation potential and highly gas-prone [25].

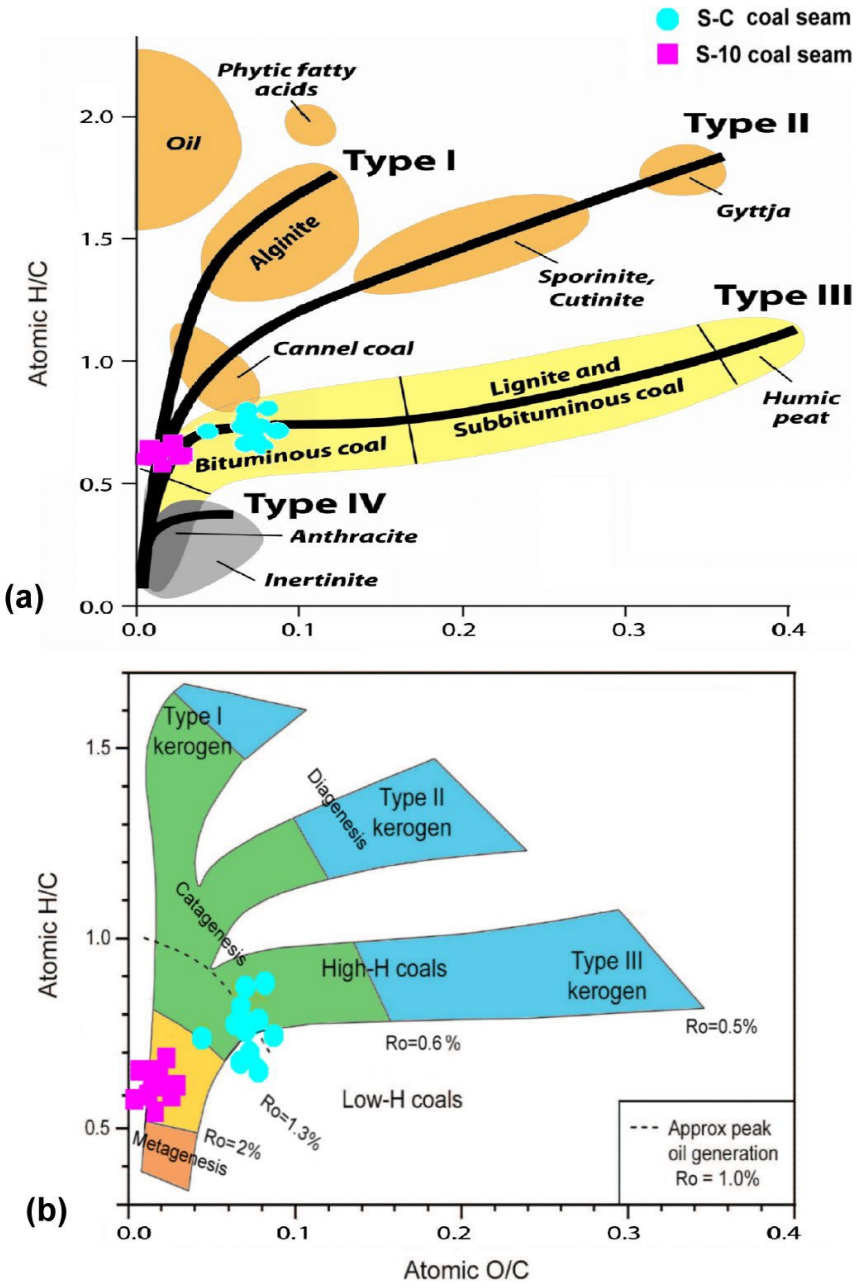

Fig. 4. H/C versus O/C modified Van-Krevelin Diagram [25, 30]

The studied coal samples of both coal seams S10 and SC lie within the type III kerogen (Fig.4 a and b). According to [25] the studied coal samples came from the pre-courser of type III kerogen that initiated from humic peat origin (Fig. 4a). All samples of S10 coal seam are laying within the late stage of cytogenesis proceed the dashed line of 1.3% vitrinite reflectance (Ro) and below the dashed line of 2% Ro that related to wet gas generation where the SC coal samples are occupied around the line of Ro equal 1% within the catagenesis stags of liquid hydrocarbon generation (Fig. 4b).

3.1.4. C/N ratio

The C/N ratio of the (S10) coal samples varies between 68.54 and 133 with an average equals to 88.9 while the C/N values of the (SC) coal samples range between 67.92 and 83.03 with an average equals to 75.35. Terrestrial OM is traditionally the richest material in the C/N ratio, they often display values between 30 and 60 more than the OM which accumulates from the marine origin [31-33]. The C/N ratio measured from the studied (S10) and (SC) coal samples show relatively very high values of an average varies from 88.89% to 75.35% in the respective order that attributed to the origin of the studied coal from a terrestrial vascular plant.

3.1.5. Gross calorific values

The calorific value mainly indicates the content of combustible elements (carbon and hydrogen). The results of the GCV of the (S10) coal samples possess an average value of 34.3 MJ/kg. Whereas, the (SC) coal samples have an average GCV value of 35.2MJ/kg (Table 2).

3.1.6. Coal rank

Based on the obtained above-mentioned results from the proximate and ultimate analysis of the (S10) and (SC) coal samples, the (S10) coal seam can be classified according to its average amount of fixed carbon (80.7% dmmf) and the volatile matter (19.3% dmmf) on the ASTM standard [34] as a bituminous group of low-volatile bituminous class. The other (SC) coal seam is considered belonging to the bituminous group of high-volatile class (A) attributed to their fixed carbon of 68.86% (dmmf) and volatile matter 31.14% (dmmf). The limits of low-volatile bituminous coal in ASTM classification are within values of 14%-22% VM and 86%-78% fixed carbon (dmmf), where the high volatile bituminous A class in the ASTM characterized by VM>31% and fixed carbon <69% (dmmf) [34].

3.2. Ash mineralogy

3.2.1. XRD mineralogical composition

The powder X-ray diffraction (XRD) is probably the most utilized method both for semi-quantitative determination of minerals in coal [35-36]. The disadvantage of XRD is the low detection limit, especially for the determination of minerals with low ash content [37]. Therefore, the analyses are usually performed on ashes at 370°C to permit a breakdown of minerals at high temperatures (Fig. 5).

Graphite is observed in both coal samples represents by 27% to 40% from coal seams S10 to SC respectively recorded as a relic of fixed carbon that transforms to end product of graphite mineral by heating during the ashing process. The quartz minerals are present in coal seam (S10) with 40% and (SC) coal by 35%. The quartz in coal may be represented by fragments that are clearly of detrital introduced into the peat swamp during peat formation [38]. According to [39] the origin of the silica that formed the quartz is not always clear; it may, for example, have been released from siliceous phytoliths within the peat-forming plant tissues and/or derived from leaching of the igneous rocks, or leaching of volcanic ash admixed with the peat accumulation. The kaolinite represents the second major mineral of 22% to 25% in S10 and SC in respective order. Kaolinite may have been introduced in situ by flocculation out of swamp waters, or by the breakdown of other minerals that may refer as an indicator of intense chemical weathering of parent rock surrounding catchments area of mire giving a coal ashing rich of kaolinite-quartz assemblage [40]. The other accessory minerals of calcite, ankerite and illite

are recorded only in the S10 coal seams with percentages range between 3%-5%. The occurrence of illite in coal is rarely found interstratified with other clay minerals reflects mostly low input of detrital minerals into the mire system. The carbonate minerals of calcite and ankerite in coal may represent autogenic origin precipitated on infilling pores and nodules or cleat, and fractures filling of epigenetic nature [41].

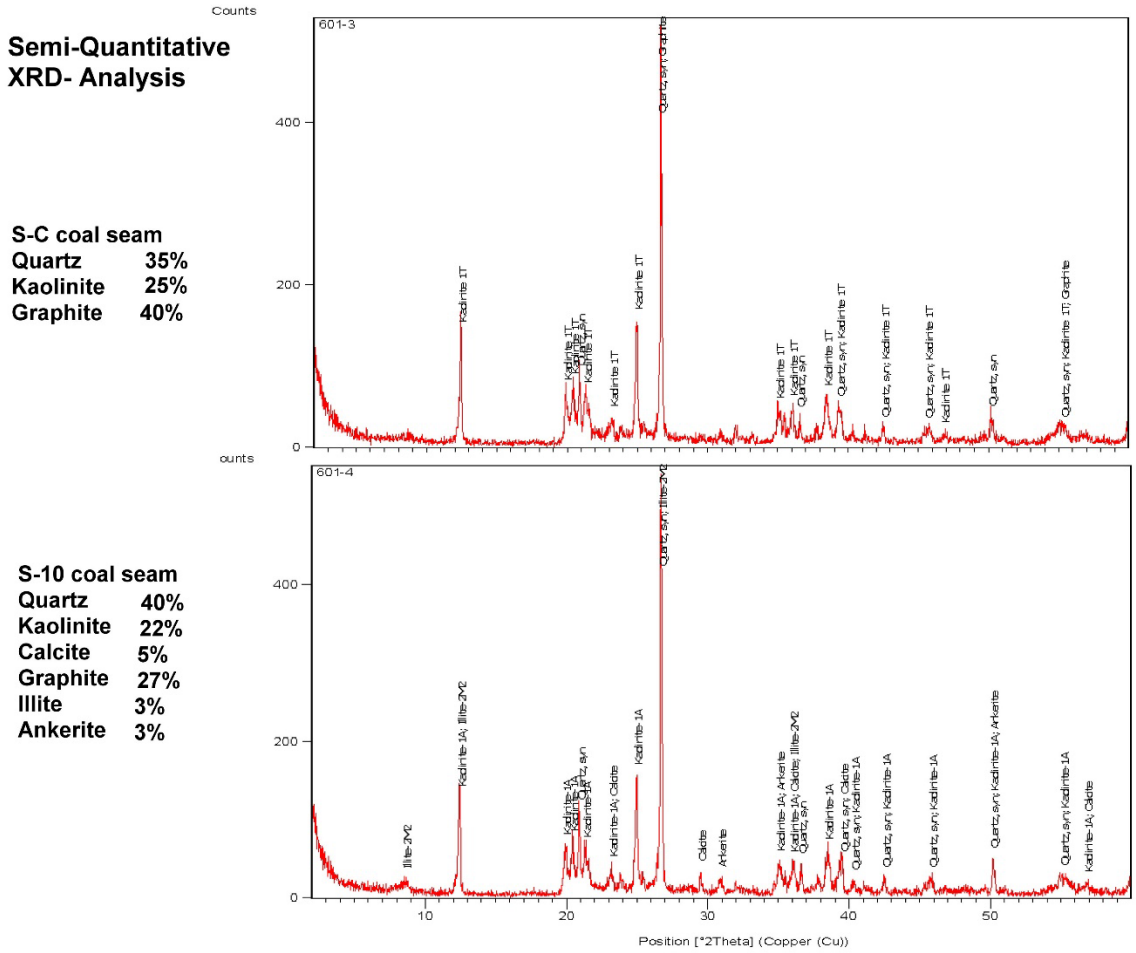

Fig. 5. Semi-quantitative of dominated minerals in ash contents of S10 and SC coal seams

3.2.2. Associations of major elements in the coal seams

The proportions of inorganic elements (reported as oxides) in the coal ashes at high temperature (815°C), derived from XRF analysis, are given in Table 3. The major oxides of the ash samples For SC samples are mainly represented by large proportions of SiO_2, Al_2O_3, with an average of 58.9% and 29.1% respectively accounting a 90% of ash mass for most of the samples, with lesser but still significant proportions of Fe_2O_3 (2.47%), CaO (1.9%), P_2O_5 (1.63%), TiO_2 (1.5%), SO_3 (1.2%) and MgO (1.04%). Other oxides, K_2O (0.91%), MnO (0.41%), and Na_2O (0.16%), each makeup less than 1% of the coal ash samples. The contents of the major oxides follow the order SiO_2>Al_2O_3>Fe_2O_3>CaO>MgO>K2O>Na_2O.

It is pertinent to mention that SiO_2 has dominant abundance followed by Al_2O_3, and the sum of SiO_2, Al_2O_3, and Fe_2O_3 contributes about 90% from the feed coal composition.

Overall, the chemical composition of all the two ash samples was similar with a slight variation of SiO_2 content (59%-57%), Fe_2O_3 content (2.47%-3.9%), CaO content (1.9%-2.38%), Na_2O content (0.16%-0.07%) and K_2O content (0.9%-0.55%). No significant variations in

these concentrations occur between the two studied coal seams. Major oxides for S10 samples do not differ from upper coal seam SC despite the difference in ash percentage between them, which indicates the same mineral source.

Our studied samples are characterized by a high SiO_2/Al_2O_3 ratio of 2.1 in SC and 1.89 in S10 (Table 3), which is higher than the theoretical SiO_2/Al_2O_3 ratio of kaolinite 1.18 [42] this high ratio coincides with the obtained results from XRD reflecting a high quartz content associated with kaolinite minerals in both coal ashes. Cross-plots of SiO_2/Al_2O_3 versus K_2O/Na_2O established by [43] applied in the present study to determine the general tectonic setting of the studied coal mire system (Fig. 6)

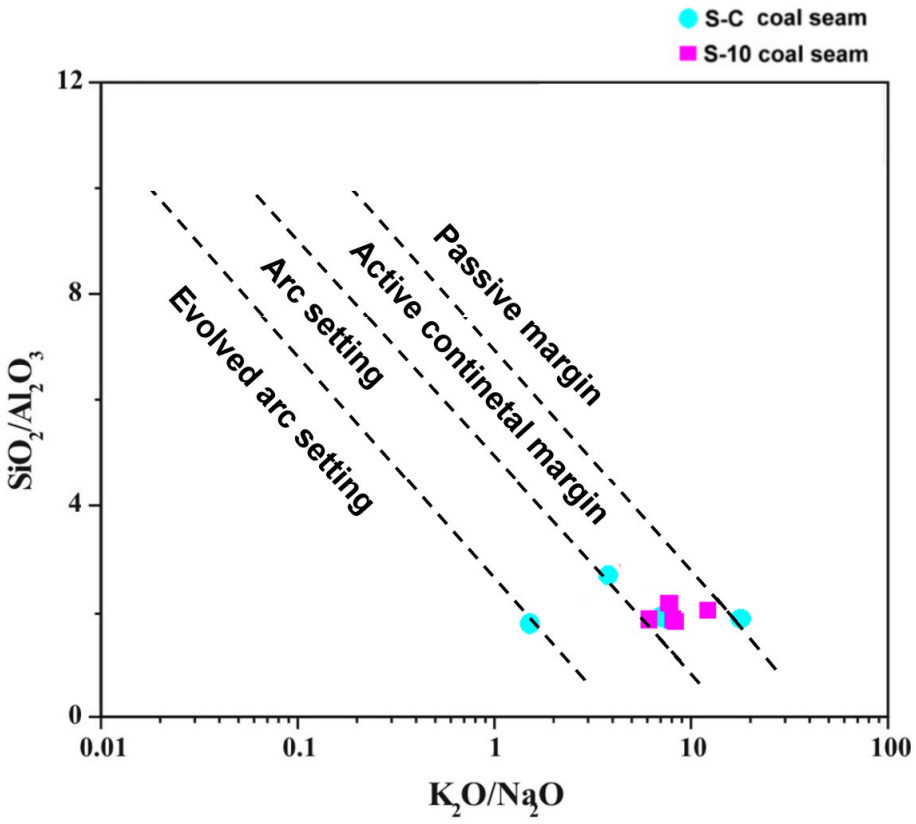

Fig. 6. Tectonic setting of major mire system [43].

The plotted samples lay dominantly within the active continental margin setting where the foreland basin may cover by vast coal-forming swamps of major-mire systems.

The ratio of TiO_2/Al_2O_3 is a useful indicator of detrital sedimentary rocks because of their stability of Ti and Al during the weathering process. The TiO_2/Al_2O_3 values for felsic, intermediate, and mafic igneous rocks are <0.02, 0.02-0.08 and >0.08 [42]. In the studied seams SC and S10, ash samples with TiO_2/Al_2O_3 values are 0.053 and 0.055, respectively. The values are lying between 0.02 and 0.07 that can be grouped to indicate intermediate ash material. The same results are obtained by plotting of S10 and SC coal samples on the chemical index of alteration (CIA) versus index of compositional variability (ICV) diagram [44] (Fig. 7a).

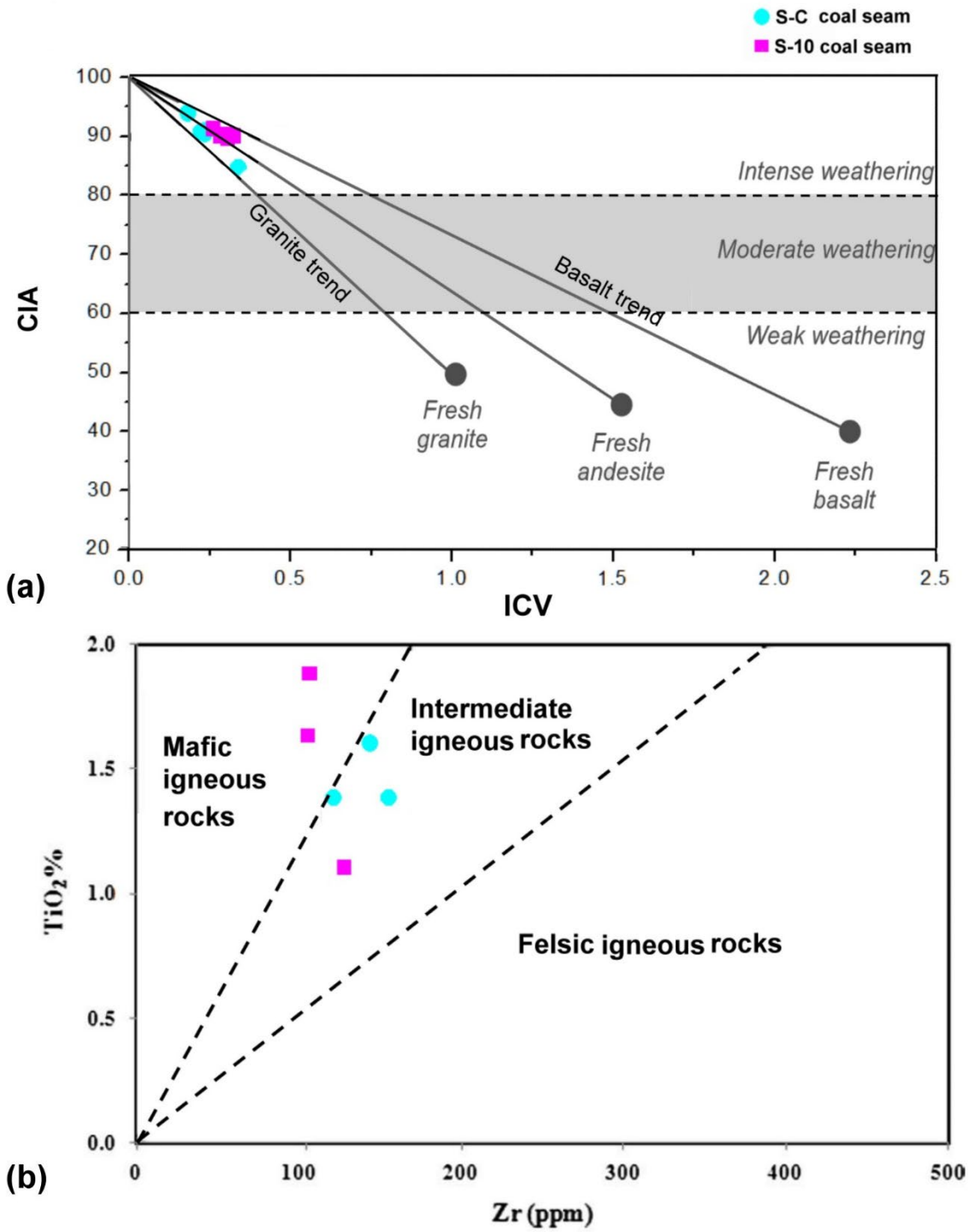

Fig. 7. General precursor parent rock of coal ash a) CIA versus ICV diagram [44]; b) TiO2 versus Zr diagram [45]

According to [46] the ICV values can give an idea of maturity of ash samples. [46] suggested that the ICV<1 indicated an optimal mature mineral of the ash. Values of CIA may reflect the intensity of weathering in the former mire and surrounding provinces. The CIA >80 indicates the intensity of chemical weathering that took place at the site of the mire and/or surrounding area [47]. The position of samples within the diagrams shows an optimal intensity of chemical

weathering during the formation of the mire system. Both figures of 7a and 7b reveal the intermediate and mafic parent igneous rock that responsible for the origin of the present ash.

The Na/K ratio could be used as an indicator of the rate of sedimentation in coal-bearing sequences [48]. The slow accumulation of sediment results in the degradation of illite and an increase in the Na/K ratio. While a rapid rate of sedimentation is reflected in a reduced Na/K ratio. Low Na/K ratios of studied samples of two coal seams are between averages of 0.12 of S10 to 0.24 of SC coal ash (Table 3) that considered an intermediate rate of sedimentation of the big mire that represented by Na/K ratio between 0.1 to 1 while the fast sedimentation rate and low sedimentation rate have values of Na/K ratios of < 0.1 and > 1 in respective order.

3.2.3. Selected trace elements in coal samples

Eighteen trace elements were analyzed by X-ray fluorescence equipment. They are (V, Cr, Ni, Cu, Zn, Y, Rb, Sr, Zr, Ba, La, Co, Pb, Th, Sn, Se, B and As) in six analysis samples represent the top, middle and base of each studied coal seams (S10 and SC). The average contents of these elements in the present studied coal seams are all within and most world coals [49] (Table 4).

From a genetic point of view, trace elements in coals in the present study are used to provide geologic information about depositional conditions associated with peat accumulation, because their distributions resulted from the processes associated with the creation of peat in the mire system.

A cross plot of TiO_2 versus Zn of the studied coal samples, as shown in Figure 7b, shows the dominated igneous rock from which coal ashes are provided. The samples indicated the dominance of mafic and intermediate Igneous rock within the major mire setting.

An important indicator of palaeoclimatology is provided from Rb/Sr and Sr/Cu ratios, according to [50]. The Sr/Cu ratio increase with increasing aridity and decreases with increasing humidity. While Rb/Sr indicates a cold-warm environment, the lowest values of it generally related to just warm conditions. The samples of S10 and SC coal seams that have Sr/Cu values <5 are laying within the area of a warm fully humid climate (Fig. 8).

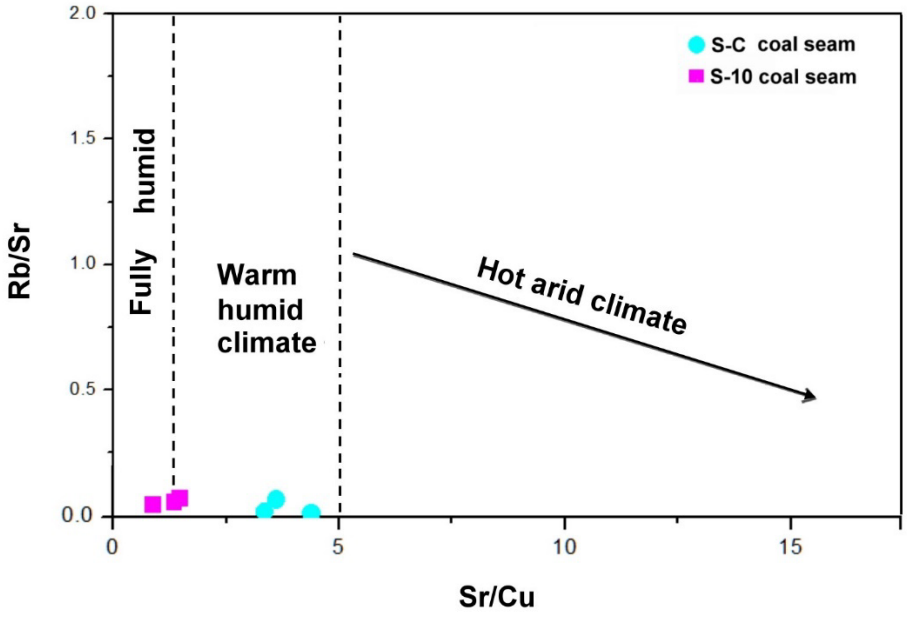

Fig. 8. The cross plot of Rb/Sr versus Sr/Cu ratios of the studied S10 and SC coal seams modified by [50]

Boron (B) in coal is mostly associated with organic matter and its concentration in coal has been used to estimate the Paleo-salinity of the depositional environment [48].

Table 3. Major oxides analysis (wt., %) of ten ash samples of the (SC) and (S10) coal seams and some of important ratios; Loss of ignition (LOI); Chemical index of alteration (CIA); Index of compositional variability (ICV)

Coal seams	Sample no.	Ash, db (815°C)	SiO_2	Al_2O_3	TiO_2	Fe_2O_3	CaO	MgO	MnO	Na_2O	K_2O	P_2O_5	SO_3	LOI	SiO_2/Al_2O_3	K_2O/Al_2O_3	TiO_2/Al_2O_3	CIA	ICV	Na_2O/K_2O	K_2O/Na_2O
(SC)	12	11.0	57.1	30	1.39	2.4	1.93	0.97	0.4	0.05	0.93	1.6	1.26	1.97	1.9	0.03	0.05	91.2	0.22	0.05	18.6
	10	7.9	58.1	29.9	1.64	2.72	1.51	1.04	0.37	0.16	1.18	1.54	1.32	0.52	1.94	0.04	0.055	91.3	0.23	0.14	7.37
	7	8.26	57.5	31.8	1.61	2.36	1.49	1.11	0.40	0.16	0.25	1.92	1.52	+0.1	1.81	0.01	0.05	94.4	0.18	0.64	1.56
	4	9.0	57.2	30.2	1.55	2.5	1.98	1.04	0.42	0.12	0.95	1.68	1.40	0,96	1.89	0.03	0.05	90.8	0.23	0.13	7.92
	1	8.82	64.8	23.7	1.39	2.36	2.6	1.04	0.46	0.32	1.26	1.4	0.52	0.04	2.7	0.05	0.06	85	0.34	0.25	3.94
Average		9.0	58.9	29.1	1.5	2.47	1.9	1.04	0.41	0.16	0.91	1.63	1.2	0.68	2.1	0.03	0.053	90.5	0.24	0.24	5.64
(S10)	9	13.1	58.5	28.4	1.89	3.68	2.34	0.93	0.37	0.05	0.63	0.82	1.05	1.32	2.06	0.02	0.067	90.4	0.28	0.08	12.6
	7	11.5	56.3	30.5	1.60	3.77	2.28	0.98	0.38	0.05	0.43	1.16	1.12	1.46	1.85	0.01	0.05	91.7	0.26	0.12	8.6
	5	11.2	55.8	29.6	1.64	4.05	2.58	1.14	0.49	0.1	0.63	0.98	1.2	1.82	1.89	0.02	0.055	89.9	0.30	0.16	6.3
	3	13.7	58.2	26.5	1.7	3.8	2.1	1.02	0.41	0.07	0.56	0.79	1.1	3.75	2.2	0.02	0.058	90.7	0.30	0.13	8
	1	11.4	56.0	29.7	1.11	4.16	2.59	1.77	0.49	0.06	0.50	0.75	1.18	1.63	1.88	0.02	0.43	90.4	0.32	0.12	8.33
Average		12.18	57.0	28.9	1.59	3.9	2.38	1.17	0.43	0.07	0.55	0.9	1.13	2.0	1.98	0.02	0.055	90.6	0.29	0.12	8.33

Table 4. Selected trace elements analysis of six samples of (S10) and (SC) coal seams and few important ratios

Coal seams	Sample no.	V	Cr	Ni	Cu	Zn	Y	Rb	Sr	Zr	Ba	La	Co	Pb	Th	Sn	Se	B	As	Rb/Sr	Sr/Cu	V/Cr	V+Ni
(SC)	12	120	34	73	139	66	6	7	468	116	200	15	11.2	4.3	4.22	11	1.4	46	3.5	0.01	3.37	3.5	193
	4	185	36	84	114	98	2	6	501	137	214	14	12.5	2.4	4.67	12	2.1	35	2.8	0.01	4.39	5.1	269
	1	266	59	95	132	127	5	27	478	148	303	18	11.2	3.0	3.76	12	3.7	32	2.2	0.06	3.62	4.5	361
	avg	190	43	84	128	97	4.3	13	482	134	239	15.7	11.6	3.2	4.22	11.6	2.4	37.7	2.8	0.03	3.76	4.4	274.33
(S10)	9	175	18	31	100	37	7	9	148	102	222	14	9.2	8.7	3.13	10	1.7	38	2.8	0.06	1.48	9.7	206
	5	162	24	34	110	45	5	7	149	101	183	14	9.9	2.8	3.40	10	0.5	25	2.0	0.04	1.35	6.8	196
	1	191	18	37	174	60	2	6	154	122	342	20	10.5	3.9	3.87	14	1.5	17	1.9	0.03	0.89	11	230
	avg	176	20	34	128	47	4.7	7.3	150	108	249	16	9.8	5.1	3.4	11.3	1.2	26.6	2.2	0.05	1.17	9	210.67

[51] showed that the degree of marine influence on coal could be inferred from the (B) content. They proposed the divisions of 50 ppm, 50–110 ppm and 110 ppm (B) to indicate freshwater influenced, mildly brackish water influenced, and brackish water influenced coals, respectively. The average born concentration in the studied S10 samples is 26.6 ppm and in the SC samples is 37.7 ppm which are low refer to freshwater origin.

Chromium (Cr) in coal is mostly associated with organic matter as Cr^{+3} especially with the clay minerals in the organic fraction of coal [52] An average concentration of Cr in S10 samples is 20 mg/kg increase up-section in SC samples to 43 mg/kg. Cr is an element that is more concentrated in coal deposited in fresh water than in coal deposited in a brackish environment [52]. Plotted of Cr versus ash contents and V+Ni for S10 and SC coal samples according to [48, 52] (Fig. 9) show that water quality during the peat accumulation is sole of freshwater that nearly of riverine and/or rain feeding. Where the redox potential in the swamp mire system is generally suboxic to dysoxic environments. The V/Cr ratio may also refer to redox potential in the mire system according to [53]. They suggested the V/Cr ratio < 2 refers to oxic; 2-4.25 of dysoxic; and > 4.25 is suboxic and anoxic. The V/Cr ratio for the studied coal is ranged from 3.5 to 11 that confirm the aquatic system of mire between suboxic and dysoxic conditions.

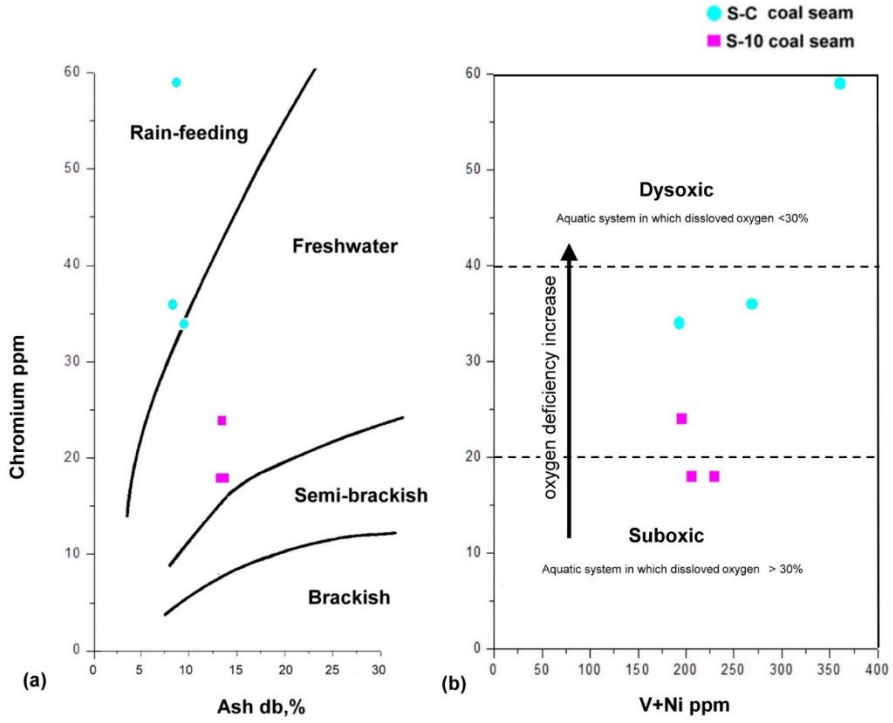

Fig. 9. Water quality and oxygen deficiency in an aquatic system in S10 and SC coal seams. a) Chromium versus ash contents b) Chromium versus V+Ni contents

4. Conclusions

The geochemical analysis postulates the studied coal seams are of medium and low grade of low volatile bituminous (S10) and high volatile bituminous (SC) coal seams. The organic components of coal belong to kerogen of type III that originate from humic matter. The vegetation of the mire system is characterized by high C/N ratios of mainly arborescent and woody vegetation with considerable amounts. The ash contents mainly composed of kaolinite and quartz minerals. The rate of sedimentary fluxes intermediate. The major mire system is within the active tectonic setting. The source of ash mineral is from the parent igneous rock of intermediate and mafic components. The palaeoclimatology was a warm humin climate. The water feeding within the mire system is only the freshwater origin either from rainfall or river systems. The aquatic redox potential within the mire is suboxic to dysoxic in which oxygen reaches minimal amounts during the former peat accumulation.

Acknowledgements

Authors appreciate and thank the TRL, the owner of Elk-View mine, Crowsnest Coalfield, for permitting collecting the studied coal samples from the operation site and allowing the present research based on the obtained results.

References

[1] Walker S: Major coalfields of the world, IEA Coal Research, 2000.
[2] Cant DJ, Stockmal GS: The Alberta foreland basin: relationship between stratigraphy and cordilleran terrane accretion events. Canadian Journal of Earth Science, 1989; 26: 1964-1975.
[3] Hacquebard PA, Cameron AR: Distribution and coalification patterns in Canadian bituminous and anthracite coals. Int. J. Coal Geol., 1989; 13: 207-260.
[4] Stone K. Coal Canadian Minerals Yearbook, 2004; 20, 1-12 (http://www.coal.ca/ content/images/stories/documents/coalreport.pdf).
[5] Smith GG, Cameron AR, Bustin RM: Coal Resources of the Western Canada Sedimentary Basin, Geological Atlas of the Western Canada Sedimentary Basin, Chapter 33. 1994.
[6] Ryan BD: Pseudovitrinite: Possible Implications for Gas Saturation in Coals and Surrounding RocksBritish Columbia Geological Survey, Geological Fieldwork 2002. 2003, 1: 203-211.
[7] Gentzis T, Deisman N, Chalaturnyk RJ: Geomechanical properties and permeability of coals from the foothills and mountain regions of western Canada. International Journal of Coal Geology, 2007; 69: 153-164.
[8] Gibson DW. Stratigraphy, sedimentology and depositional environments of the coal-bearing Jurassic-Cretaceous Kootenay Group, Alberta and British Columbia. Geological Society Canada Bulletin, 1985; 357: 1-108.
[9] Bustin RM, Smith GG Coal deposits in the front ranges and foothills of the Canadian Rocky Mountains, southern Canadian Cordillera. International Journal of Coal Geology, 1993; 23: 1-27.
[10] Vessey SJ, Bustin RM: Sedimentology of the coal-bearing Mist Mountain Formation, Line Creek, Southern Canadian Cordillera: relationships to coal quality, Int. J. Coal Geol., 2000; 42: 129-158.
[11] Kalkreuth WD. Coal facies studies in Canada, Int. J. of C. Geol., 2004; 58: 23-30.
[12] Goodarzi F, Grieve DA, Sanei H, Gentzis T, Goodarzi NN. Geochemistry of coals from the Elk Valley coalfield, British Columbia, Canada. Int. J. Coal. Geol. 2009; 77: 246-259.
[13] Pearson DE, Grieve DA. Rank variation, coalification patterns and coal quality in the Crowsnest coalfield British Columbia. The Canadian Mining and Metallurgical Bulletin, September, 1985; 39-46.
[14] Bustin RM, England TDJ. Timing of organic maturation (coalification) relative to thrust faulting in the southeastern Canadian Cordillera. Int. J. Coal Geol., 1989; 13: 327-339.
[15] Grieve DA. Coal fields of the East Kootenay region, southeastern British Columbia. In: Patching TH (ed) Coal in Canada. Can Inst Min Metall, 1985; 31, 203-211.
[16] British Columbia Coal Industry Overview (BCCIO). https://www2.gov.bc.ca/gov/content/industry/mineral-exploration-mining/british-columbia-geologicalsurvey/publications. 2018
[17] ISO-562. Hard Coal and Coke. Determination of Volatile Matter. International Organization for Standardization, Geneva. Switzerland, 2010.
[18] ISO-1171. Solid Mineral Fuels, Determination of Ash Content. International Organization for Standardization, Geneva. Switzerland, 2010.
[19] ASTM D-4239. Standard Test Method for Sulfur in the Analysis Sample of Coal and Coke Using High-Temperature Tube Furnace Combustion Methods, 2020.
[20] Sun R, Guijian L, Zheng L, Choul CL. Characteristics of coal quality and their relationship with coal-forming environment: a case study from the Zhuji exploration area, Huainan coal field, Anhui, China. Energy. 2010; 35 (1): 423-435.
[21] Sivek M, Sedláčková L, Jirásek J, Čáslavský M. Variation of moisture content of the bituminous coals with depth: A case study from the Czech part of the Upper Silesian Coal Basin Int. J. of Coal Geology. 2010; 84: 16-24.
[22] Speight JG. Chemistry and Technology of coal, CRC Press Taylor & Francis Group, 2013.
[23] Edress NAA, Attia GM, Abdel-Fatah AR. Construct a Paleo-limnological environment based on coal petrography; case study, two selected coal seams, north Crowsnest open-pit mine, Canada, , Iraqi Geological Journal, 2021; 54(2D). (in press)
[24] Diessel CFK. Coal-bearing depositional systems, Springer, Berlin, 1992a; 721 pp.
[25] Suarez-Ruiz I, Crelling JC. Applied coal petrology: The role of petrology in coal utilization. Coal Combustion, I. Suarez-Ruiz and J.C. Ward (Eds.). Elsevier, Amsterdam, the Netherlands, 2008

[26] Chou CL. Sulfur in coals: A review of geochemistry and origins. International Journal of Coal Geology, 2012; 100: 1-13.
[27] Wüst RAJ,. Ward CR, Bustin RM, Hawke MI. Characterization and quantification of inorganic constituents of tropical peats and organic-rich deposits from Tasek Bera (Peninsular Malaysia): implications for coals, International Journal of Coal Geology, 2002; 49: 215-249.
[28] Ward CR, Li Z, Gurba LW. Variations in elemental composition of macerals with vitrinite reflectance and organic sulphur in the Greta Coal Measures, New South Wales, Australia, International Journal of Coal Geology, 2007; 69: 205-219.
[29] Edress NAA. Coalification, coal facies and depositional environment of the 9th to 12th coal seams of the Jan Šverma Mine Group, Lampertice Member (IntraSudetic Basin, Czech Republic) from the view point of coal petrology, Ph.D. Thesis, Karlova Uni. v Praze, Czech Republic. 2007.
[30] Gaupp R, Möller P, Lüders V, di Primio R, Littke R. Fluids in sedimentary basins: an overview. 2008, Springer. https://link.springer.com/content/pdf/10.1007%2 F978-3-540-85085-4_6.pdf
[31] Twichell SC, Meyers PA, Haass LD. Significance of high C/N ratios in organic carbon-rich Neogene sediments under the Benguela Current upwelling system. Organic Geochemistry, 2002; 33, 715-722.
[32] Mc-Groddy ME, Daufresne T, Hedin LO. Scaling of C:N:P stoichiometry in forests worldwide: implications of terrestrial redfield-type ratios. Ecology, 2004; 85 (9): 2390-2401.
[33] Liu Q, Liang Y, Cai W, Wang K, Wang J, Yin K. Changing riverine organic C: N ratios along the Pearl River: Implications for estuarine and coastal carbon cycles, Science of the Total Environment, 2020; 709, 1-10.
[34] ASTM D-388-99: Standard Classification of Coal by Rank. The American Society for Testing and Materials, 100Barr Harbor Drive, PO Box C700, West Conshohocken, United States, 2016.
[35] Ward CR, Matulis CE, Taylor JC, Dale LS.. Quantification of mineral matter in Argonne Premium Coals using interactive Rietveld-based X-ray diffraction. Int. J. Coal Geol., 2001a; 46: 67-82.
[36] Ward CR, Spears DA, Booth CA, Staton I, Gurba LW. Mineral matter and trace elements in coals of the Gunnedah Basin, New South Wales, Australia. Int. J. Coal Geol., 1999; 40: 281–308.
[37] Wertz DL. X-ray analysis of the Argonne premium coals: 1. Use of absorption/diffraction methods. Energy Fuels, 1990; 4: 442-447.
[38] Wüst R, Bustin RM, Ross J. Neo-mineral formation during artificial coalification of low-ash - mineral free-peat material from tropical Malaysia-potential explanation for low ash coals. Int. J. Coal Geol., 2008' 74, 114-122
[39] Ward CR, Crouch A, Cohen DR. Identification of potential for methane ignition by rock friction in Australian coal mines. Int. J. Coal Geol., 2001b; 45: 91-103.
[40] Beaton AP, Goodarzi F, Potter J. The petrography, mineralogy and geochemistry of a Paleocene lignite from southern Saskatchewan, Canada. Int. J, Coal. Geol., 1991; 17: 117-148.
[41] Pinetown KL, Ward CR, van der Westhuizen WA. Quantitative evaluation of minerals in coal deposits in the Witbank and Highveld Coalfields and the potential impact on acid mine drainage. Int. J. Coal Geol.; 2007; 70: 166-183.
[42] Li J, Zhang M, Li B, Monteiro SN, Ikhmayies SJ, Kalay YE, Hwang J, Escobedo-Diaz JP, Carpenter JS, Brown AD, Soman R, Moser A. (Eds.) Characterization of Minerals, Metals, and Materials, The Minerals, Metals & Materials Series, Springer Nature., 2021; 613p.
[43] Floyd PA, Winchester JA, Park RG. Geochemistry and tectonic setting of Lewisian clastic metasediments from the Early Proterozoic Loch Maree Group of Gairloch, NW Scotland. Precambr. Res., 1989; 45: 203-214.
[44] Lee YI. Provenance derived from the geochemistry of late Paleozoic–early Mesozoic mudrocks of the Pyeongan Supergroup, Korea. Sediment. Geol., 2002; 149: 219-235.
[45] Hayashi K, Hiroyuki F, Heinrich HD, Ohmoto H. Geochemistry of 1.9 Ga sedimentary rocks from northeastern Labrador, Canada. Geochimica et Cosmochimica Acta, 1997; 61: 4115-4137.
[46] Cox R, Lowe DR, Cullers RL. The influence of sediment recycling and basement composition on evolution of mudrock chemistry in the southwestern United States. Geochim. Cosmochim. Acta, 1995; 59: 2919-2940.
[47] Dai S, Wang X, Zhou Y, Hower JC. Li D, Chen W, Zhu X, Zou J. Chemical and mineralogical compositions of silicic, mafic, and alkali tonsteins in the Late Permian coals from the Songzao Coalfield, Chongqing, Southwest China. Chem. Geol., 2011; 282: 29-44.

[48] Goodarzi F, Goodarzi NN, Malachowska A. Elemental composition, environment of deposition of the lower Carboniferous Emma Fiord formation oil shale in Arctic Canada. I. Journal of Coal Geology., 2021; 244(132): 103 715.
[49] Swine DJ. A Trace Elements in Coal. Buttrerworths, London, 1990; 278 P.
[50] Mikheeva EA, Demonterova EI, Ivanov AV. Geochemistry of the Cheremkhovo and Lower Prisayan Formations from the Jurassic Irkutsk Coal-Bearing Basin: Evidence for Provenance and Climate Change in Pliensbachian-Toarcian, Minerals, 2021; 11, 357
[51] Goodarzi F, Swaine DJ. The influence of geological factors on the concentration of boron in Australian and Canadian coals. Chemical Geology, 1994; 118: 301-318.
[52] Goodarzi F, Van Der Flier-Keller E. Distribution of major, minor and trace elements in Hat Creek Deposit No. 2, British Columbia, Canada. Chemical Geology, 1988; 70: 313-333.
[53] Jones B, Manning DAC. Comparison of geochemical indices used for the interpretation of palaeoredox conditions in ancient mudstones, Chemical Geology, 1994; 111: 111-129

To whom correspondence should be addressed: Dr. Nader A. A. Edress, Geology Department, Faculty of Sciences, Helwan University, Cairo, Egypt, E-mail: ; nedress@outlook.com; nedress@science.helwan.edu.eg
Orcid: 0000-0002-7320-486X